NOAAGlobalTemp version 6: An AI-based global surface temperature dataset

Xungang Yin[1*], Boyin Huang[1], Matthew Menne[1], Russell Vose[1], Huai-Min Zhang[1], Adedoja Adeyeye[1], Scott Applequist[1], Karin Gleason[1], Chunying Liu[2], Ahira Sanchez-Lugo[1]

[1] NOAA National Centers for Environmental Information, Asheville, North Carolina
[2] Riverside Technology, Inc., Asheville, North Carolina

[*] Corresponding author email address: Xungang.Yin@noaa.gov

(Submitted to **Bulletin of the American Meteorological Society**)

Early Online Release: This preliminary version has been accepted for publication in *Bulletin of the American Meteorological Society*, may be fully cited, and has been assigned DOI 10.1175/BAMS-D-24-0012.1. The final typeset copyedited article will replace the EOR at the above DOI when it is published.

Abstract

The National Oceanic and Atmospheric Administration (NOAA) Global Surface Temperature (NOAAGlobalTemp) dataset is widely used for scientific research, operational monitoring, and climate assessment activities. Aligning with NOAA's mission values, NOAAGlobalTemp has been updated to version 6 (i.e., NGTv6), which includes two enhancements over its predecessor (NGTv5). The first enhancement is the expansion of the spatial coverage to encompass the entire globe and the extension of temporal coverage back to 1850 (an interim version of NOAAGlobalTemp with these features was released in February 2023). The expansion of spatial coverage is accomplished by utilizing surface air temperatures over the Arctic Ocean and by eliminating the data reconstruction mask used in NGTv5 that had suppressed interpolation in data-sparse regions. This change has important implications for global temperature trends since the Arctic region has been warming at a much faster pace, more than four times the global average, in the twenty-first century to date. The second enhancement is the implementation of a methodology based on artificial intelligence (AI) for reconstructing surface air temperature over the global land surface and the Arctic Ocean. The AI model employs an artificial neural network to fill data gaps and is demonstrated to be more robust, stable, and accurate than the previous gap-filling method, particularly in observation-sparse areas such as the polar regions. The model outperforms the previous approach across all evaluated statistical metrics, and the output reaches a stable state more quickly as observations are received, which facilitates climate monitoring. NGTv6 was released in February 2024.

Keywords: NOAAGlobalTemp, climate change, climate warming, global surface temperature, artificial intelligence.

Introduction

NOAAGlobalTemp combines long-term sea surface (water) temperature (SST) and land surface air temperature (LSAT) to create a spatially complete depiction of global surface temperature anomalies and trends. The dataset provides monthly mean temperature anomalies from pre-industrial time to present using observations from a wide variety of observing networks during the era of instrumental temperature records. NOAAGlobalTemp's comprehensive spatiotemporal coverage of the Earth's surface temperature makes it one of the common data sources for

Accepted for publication in *Bulletin of the American Meteorological Society*. DOI 10.1175/BAMS-D-24-0012.1.

national and international climate assessments and reports. For example, it is used in NOAA's climate monitoring reports (https://www.ncei.noaa.gov/monitoring), World Meteorological Organization (WMO) State of the Global Climate reports (https://wmo.int/publication-series/state-of-global-climate), and United Nations Intergovernmental Panel on Climate Change (IPCC) reports (https://www.ipcc.ch/assessment-report).

In line with NOAA's mission values, the NOAAGlobalTemp data construction system has been periodically updated since its creation to incorporate increased data coverage, new observation platforms, and improved data quality, and to recognize and apply state-of-the-art knowledge and methods (Smith and Reynolds 2005; Smith et al. 2008; Vose et al. 2012; Zhang et al. 2019; Vose et al. 2021; Huang et al. 2022). Version updates may reflect improvements in underlying input data, changes of data reconstruction methodology, or both. For instance, in June 2019, we released NOAAGlobalTemp version 5 (NGTv5; Zhang et al. 2019), which used a more comprehensive data collection that increased spatial coverage over land and ocean surfaces, as well as improved treatment of historical changes in observing practice (Zhang et al 2019). Subsequently, the product team continued to pursue data improvement and algorithm development for the next generation NOAAGlobalTemp. The efforts have resulted in two version updates, first a minor version release of 5.1 (NGTv5.1), and then a major version release of 6 (NGTv6). NGTv6 has been operational since February 2024. As technical details, including changes in input data, methodologies, and output validations and comparisons, have been comprehensively described in Vose et al. (2021) and Huang et al. (2022), this paper serves as an overview of the new features in NGTv6 and the changes since the last major version, NGTv5.

About NOAAGlobalTemp version 6

NGTv6 is a monthly mean surface temperature dataset with complete global coverage. It spans the period from January 1850 to present and is updated monthly. Observations of air temperature over land and the Arctic Ocean and water surface temperature from oceans, seas and large lakes are merged and analyzed on 5-degree spatial grids. The gridded temperatures represent anomalies relative to the means for the corresponding months during 1971−2000. The purpose of using anomalies is to provide baseline data for the assessment of large-scale temperature features, particularly long-term trends. Compared to absolute temperatures, temperature anomalies have much greater spatial coherence and therefore are more suitable in describing

Accepted for publication in *Bulletin of the American Meteorological Society*. DOI 10.1175/BAMS-D-24-0012.1.

temperature variations particularly for areas with complex terrains or constantly changing observation networks.

NGTv6 receives data input from multiple sources: The Global Historical Climatology Network monthly (GHCNm; Menne et al. 2018) version 4 for LSAT; the Extended Reconstructed SST (ERSST; Huang et al. 2017) version 5 for SST; the International Comprehensive Ocean-Atmosphere Data Set (ICOADS; Freeman et al. 2017; Liu et al. 2022) and the International Arctic Buoy Programme (IABP; Rigor and Ortmeyer 2003) for Arctic Ocean surface air temperature. Over land and the Arctic Ocean, station air temperatures are averaged into grid values, but spatial coverage is not complete because some areas lack data. Consequently, NGTv6 employs an artificial intelligence (AI) model to interpolate/extrapolate observations to data-missing grids. Over water (excluding the Arctic Ocean), the input SSTs from ERSST, which are on 2-degree grids and provide complete coverage, are regridded to match the 5-degree grids. These are then merged with the gap-filled air temperatures, forming a gap-free global surface temperature dataset.

Enhancements from version 5 to 6

NGTv6 includes two incremental enhancements over the previous major version (NGTv5). The first is the expansion of the spatiotemporal coverage (Vose et al. 2021), which resulted in a minor version release (NGTv5.1) in February 2023. The second is the implementation of an AI-based methodology for surface air temperature reconstruction (Huang et al. 2022), which led to the current major version release of NGTv6.

Expanding to full global coverage

In NGTv5 and its predecessors, temperature reconstruction was masked out in a) high latitude oceans with ice concentration above 50%, and b) observation-sparse areas where the percent of grids containing observations is lower than 20% in the 25°×25° region centered at the grid in question. This criterion resulted in data gaps in regions where observing networks were not well established. In the early periods, particularly prior to the 1950s, large data-missing areas as a result of insufficient observations were frequently seen (Huang et al. 2017; Menne et al. 2018). With the gradual expansion of the global observing system, particularly after World War-II, most of the observation-sparse areas had been steadily filled except near the polar regions. The

Accepted for publication in *Bulletin of the American Meteorological Society*. DOI 10.1175/BAMS-D-24-0012.1.

average global data coverage of NGTv5 was about 80% during 1880-1950 and about 92% during 1951−2023. Since the 1950s, data gaps were primarily in the polar regions, as exhibited in the top row panels of Fig. 1, which show the NGTv5 data coverage in January and July 2023 as examples.

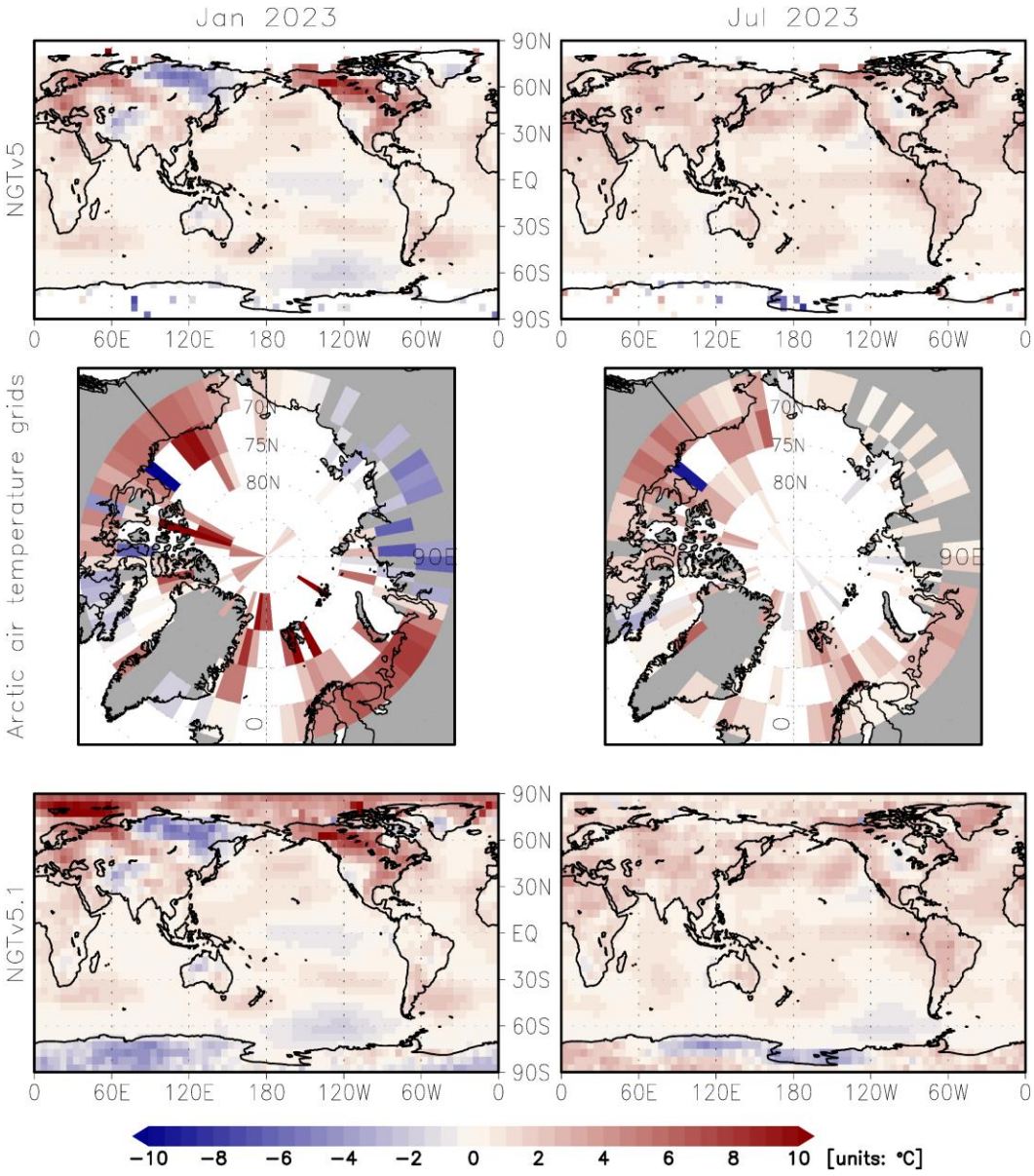

Fig. 1. NOAAGlobalTemp data coverage in January (left column) and July (right column) 2023. Top row: output of NGTv5; middle row: input data grids in the Arctic region north of 65°N in NGTv5.1; bottom row: output of NGTv5.1.

Accepted for publication in *Bulletin of the American Meteorological Society.* DOI 10.1175/BAMS-D-24-0012.1.

Although the purpose of applying a data-mask in observation-sparse areas was to minimize potential interpolation errors, the downside was that these areas were not included in regional or global assessments. For example, in the January and July 2023 NGTv5 (shown in the top row of Fig. 1), most grids in the two polar regions were masked out. Given that regions poleward of 65°N and S constitute a total of 9.4% of the global area, their exclusion can bias estimates of the global temperature average. Additionally, it has been observed that the Arctic region is warming at a much faster pace than the rest of the planet, a phenomenon known as Arctic amplification (Serreze and Barry 2011). Therefore, to accurately depict the global surface temperature change, particularly when it comes to temperature trends, it is essential to incorporate the temperatures of the two polar regions in NOAAGlobalTemp.

In NGTv5 and its prior versions, SST was used for the Arctic Ocean. However, in the Arctic Ocean, temperature variations cannot be reasonably represented by SST. This is because not only are the in situ SST observations scarce, but also a large portion of the Arctic Ocean is covered with seasonal sea ice or ice-water mixtures, whose lowest temperature is bounded by a freezing point of -1.8°C. Also, since SST and LSAT anomalies exhibit different orders of magnitude and variance, the changing ice cover over the Arctic Ocean could result in an artifact in the mean surface temperature change. Vose et al. (2021) introduced an alternative method to describe the Arctic temperature in NGTv5.1. In this approach, the aforementioned data mask was removed, and the Arctic Ocean was treated as if it were land and, thus, near surface air temperature anomalies were used instead of SST. One advantage of using surface air temperature over the Arctic Ocean is that it maintains a constant land/sea proportion, thereby avoiding the introduction of a gradual shift in the magnitude of surface temperature anomalies. In NGTv5.1, two new data sources, the ICOADS and the IABP, were added to provide surface air temperatures recorded by ships, buoys, and ice stations over the Arctic Ocean. These data were first analyzed on 5-degree grids and then merged with the gridded GHCNm LSAT to form an extended LSAT dataset. The empirical orthogonal teleconnection (EOT; Van den Dool et al. 2000) analysis, which was used to expand data coverage in NOAAGlobalTemp (Smith and Reynolds 2005), was updated with a re-defined land coverage by including additional modes representing the Arctic patterns. With the above modifications, full global coverage is achieved in NGTv5.1.

Accepted for publication in *Bulletin of the American Meteorological Society.* DOI 10.1175/BAMS-D-24-0012.1.

Before 1979, air temperature observations in the Arctic Ocean were all from ICOADS. The total number of observations was low in the early period but began to increase since the 1950s. Since 1979, with the launch of IABP, the total number of 5°×5° grids with observations from the two sources has been steadily varying between 20 and 100, contributing areal coverage between 5% and 35% of the Arctic region north of 65°N. In the examples shown in the middle row of Fig. 1, data from ICOADS and IABP covered 12% and 19% of the Arctic region in January and July 2023, respectively, complementing the GHCNm contributions.

In summary, NGTv5.1 was released in February 2023. Its primary advancements were the introduction of surface air temperature for the Arctic Ocean, the removal of the data mask leading to full spatial coverage, and extending the record back to 1850. For the examples of January and July 2023, as depicted in Fig. 1, the full coverage of NGTv5.1 (bottom row) exceeds the masked coverage of NGTv5 (upper row) by 4.7% and 6.4% for the respective two months. A comparison between NGTv5.1 and the gridded temperatures from ice mass balance (IMB) buoys, based on their common grids during 2002−2016, shows a good agreement (Fig. S1a). NGTv5.1 and IMB exhibit similar increasing trends (1.92°C vs 1.90°C per decade), and their correlation reaches 0.71 (0.68 when detrended; $p \leqslant 0.01$).

Implementation of an AI-based reconstruction algorithm over land and the Arctic Ocean

Overall, the EOT analysis employed in NGTv5.1 has proven to be effective in filling gaps and filtering noise, given relatively enough and well-distributed observations. However, the method sometimes may struggle in observation-sparse areas, as the selection of localized modes heavily relies on the spatial distribution of observations. Specifically, in a month, an EOT mode is used only if the percentage of the associated variance sampled by observations relative to the total variance of the first-guess reaches a certain level. This requirement aims to avoid noise due to inadequate sampling, but it may overlook some localized modes that could be important to a particular area, leading to a suboptimal data reconstruction. To address this issue, Huang et al. (2022) developed a new reconstruction method involving an AI-based model that uses an artificial neural network (ANN) to replace the EOT method as the problem solver. The ANN approach is employed in NGTv6, which was released in February 2024.

Accepted for publication in *Bulletin of the American Meteorological Society*. DOI 10.1175/BAMS-D-24-0012.1.

The ANN consists of three layers, namely input, hidden, and output layers. The training and validation data are the 1950−2020 surface air temperatures over the global land and the Arctic Ocean, extracted from the ECMWF Reanalysis v5 (ERA5; Hersbach et al. 2020). The model was first trained based on the data mask of the extended LSAT in each month. Then, the trained model was used to fill data gaps in corresponding months. The performance of the ANN model was assessed by comparing the ANN output with the EOT output (Huang, et al. 2022). During 1850−2020, ANN outperforms EOT in all statistical metrics including spatial correlation (0.89 vs 0.78) and root-mean-square difference (0.68 vs 0.98). The spatial variances of the extended LSAT reconstructed by ANN are higher than those reconstructed by EOT. This is particularly significant for observation-sparse areas, where EOT is known to excessively dampen the spatial variations in temperature. Huang et al. (2022) provided more details about the ANN model.

In the following, we demonstrate the superior performance of the ANN method over the EOT method using a real-time example. This example is drawn from the NGTv6 and NGTv5.1 outputs for August 2023, which were generated during the NGTv6 test operation conducted in September 2023. We use this example to show how the EOT and ANN methods responded to data delays in the Antarctic region.

Typically, we anticipate that input observations for each month will be received at the beginning of the following month. However, data from some stations can be delayed. The impacts of these delayed data may be negligible in areas with dense observing networks but can be significant otherwise. Fig. 2 displays the NOAAGlobalTemp data in Antarctica for August 2023. Columns 1−3 are the operational results generated on September 4th, 8th, and 16th, respectively. The GHCNm input, NGTv5.1 output, and NGTv6 output from the three runs are shown in rows 1−3, respectively. We focus on the region in the third quadrant of the map, which is approximately between 90°W and the Ross Sea. For the input data (top row of Fig. 2), during the first run (Sept-04), there were no observations received for the area. During the next two runs (Sept-08 and Sept-16), the number of received observations gradually increased. By the end (Sept-16), the received observations were sufficient to indicate a cold anomaly in this region. Both NGTv5.1 (middle row of Fig. 2) and NGTv6 (bottom row of Fig. 2) demonstrate that they reasonably constructed the surface temperature pattern when sufficient observations were

Accepted for publication in *Bulletin of the American Meteorological Society*. DOI 10.1175/BAMS-D-24-0012.1.

ingested, as shown by the Sept-16 run. However, while NGTv6 performs effectively even when input data was insufficient during the first two runs, NGTv5.1 produced a warm anomaly in the target area in the Sept-04 run and dampened the spatial variations over most of Antarctica in the Sept-08 run. This outcome exemplifies the robustness, stability, and accuracy of the ANN approach.

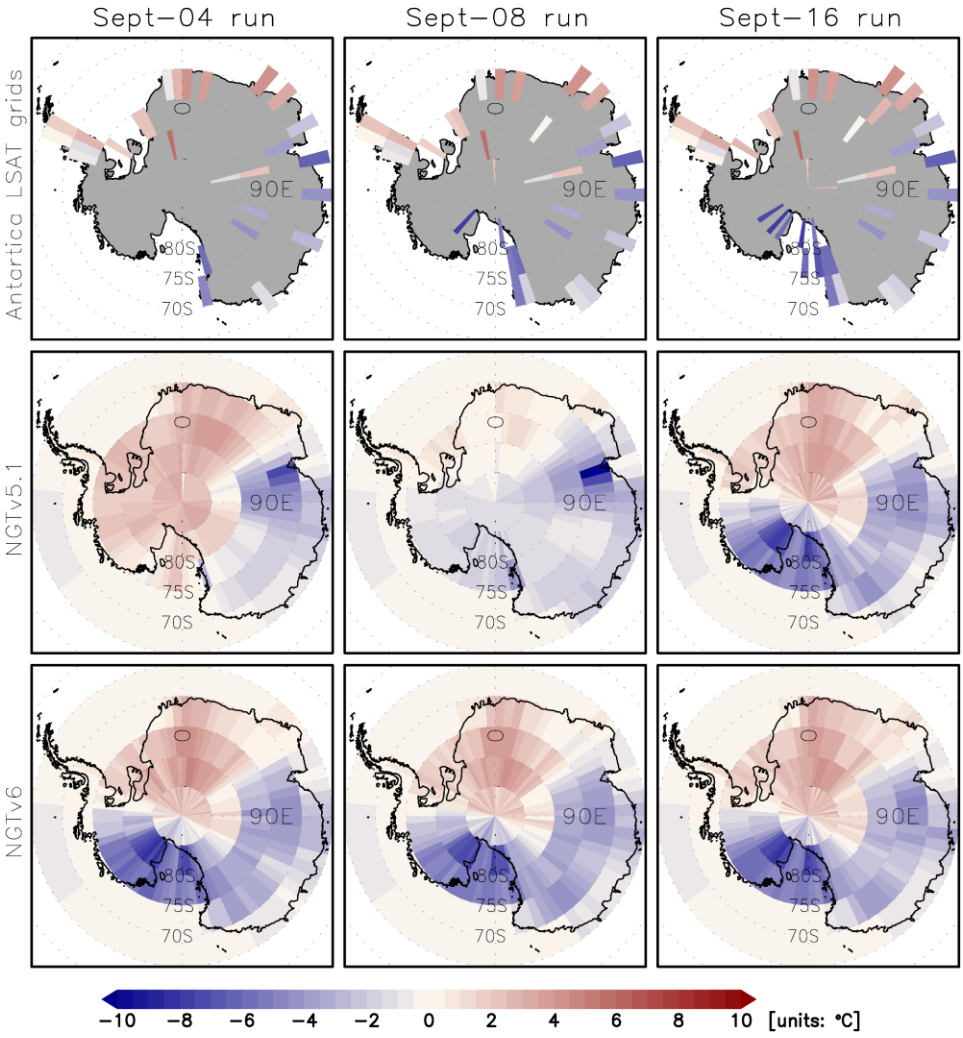

Fig. 2. Operational data for the NOAAGlobalTemp in Antarctica for August 2023, generated on September 4th, 8th, and 16th of 2023, respectively displayed in the columns from left to right. The three rows, from top to bottom, are for GHCNm input, NGTv5.1 output, and NGTv6 output.

In the Arctic region, NGTv6 is also compared with IMB temperatures in the same manner as NGTv5.1 (Fig. S1b). Based on their common grids during 2002−2016, the trend of NGTv6 is 0.208°C/decade, higher than that of NGTv5.1 (0.192°C/decade) or IMB

Accepted for publication in *Bulletin of the American Meteorological Society*. DOI 10.1175/BAMS-D-24-0012.1.

(0.190°C/decade). The correlation with IMB temperatures is higher for NGTv6 than for NGTv5.1, 0.77 vs 0.71 (0.75 vs 0.68 when detrended; $p \leqslant 0.01$), indicating an improved performance of NGTv6.

Assessment of temperature trends

One of the most important applications of NOAAGlobalTemp is the analysis of temperature trends. Specifically, both WMO and IPCC utilize NOAAGlobalTemp, among other resources, to evaluate global temperature trends and monitor the current status of temperature relative to pre-industrial levels. To assess the potential impacts of coverage and methodology changes on trends during version updates, we computed the mean surface temperatures and their trends for NGTv5, NGTv5.1, and NGTv6. These are displayed in Fig. 3. Given that NGTv5 has very limited coverage in the two polar regions, we made comparisons for both the extrapolar (65°S−65°N; upper panel of Fig. 3) and the global (90°S–90°N; lower panel of Fig. 3) regions. The trends were calculated for the periods 1850−1900 (excluding NGTv5 which starts in 1880), 1901−1950, 1951−2000, 1901−2000, and 2001−2023, as denoted in the figure. All trends after 1901, as well as the global trend in NGTv6 during 1850−1900, are statistically significant at $p \leq 0.01$. The common feature of the time series in Fig. 3 is that temperature decreased from 1850 until about 1910, followed by an increase through the early 1940s. Then, after a slight decrease through the early 1960s, temperature started to increase nearly monotonically throughout the rest of the twentieth century and continued into the twenty-first century. Both short-term and long-term variations are consistent among all versions. The twentieth century trends from all versions for both extrapolar and global regions are very close, with values between 0.073 and 0.075°C/decade. With the exception of the global trends during 1850−1900, the trends of NGTv5.1 and NGTv6 are the same or nearly the same, but they can differ from the trend of NGTv5 during certain periods. The differences among the trends of different versions are attributable to changes in coverage and/or methodology during version updates. During 1901−1950, the trend of NGTv5 was markedly different from the trends of the two later versions (0.091 vs 0.083/0.082 and 0.096 vs 0.089/0.088 respectively for extrapolar and global regions; units: °C/decade). This discrepancy is due to the sparse in situ observations over both land and ocean during that time, which resulted in large areas being masked out in NGTv5. For the extrapolar region, since the 1950s, the number of in situ observations steadily increased and thus

Accepted for publication in *Bulletin of the American Meteorological Society*. DOI 10.1175/BAMS-D-24-0012.1.

NGTv5 gained more and more coverage. As a consequence, the trends of the three versions were close as shown in the figure. For the global region, the differences in trends among versions in the beginning and end periods were much greater than those observed for the extrapolar region. During the pre-industrial era (1850−1900), when observations in the polar regions were extremely scarce, the larger difference between the NGTv5.1 trend (-0.006°C/decade) and the NGTv6 trend (-0.013°C/decade) was primarily due to the fact that the EOT method used in NGTv5.1 is incapable of capturing the variability as effectively as the ANN method used in NGTv6 in areas with sparse observations (Huang et al., 2022). For the twenty-first century to date (2001−2023), the global trends of NGTv5.1 and NGTv6 (0.228 and 0.229 °C/decade) are similar, but more than 8% greater than the trend of NGTv5 (0.211°C/decade). This reflects the contributions from the polar regions, which are largely masked out in NGTv5. In fact, the larger trends in NGTv5.1 and NGTv6 were due to the much stronger warming trend of surface air temperature in the Arctic region during recent decades (i.e., Arctic amplification).

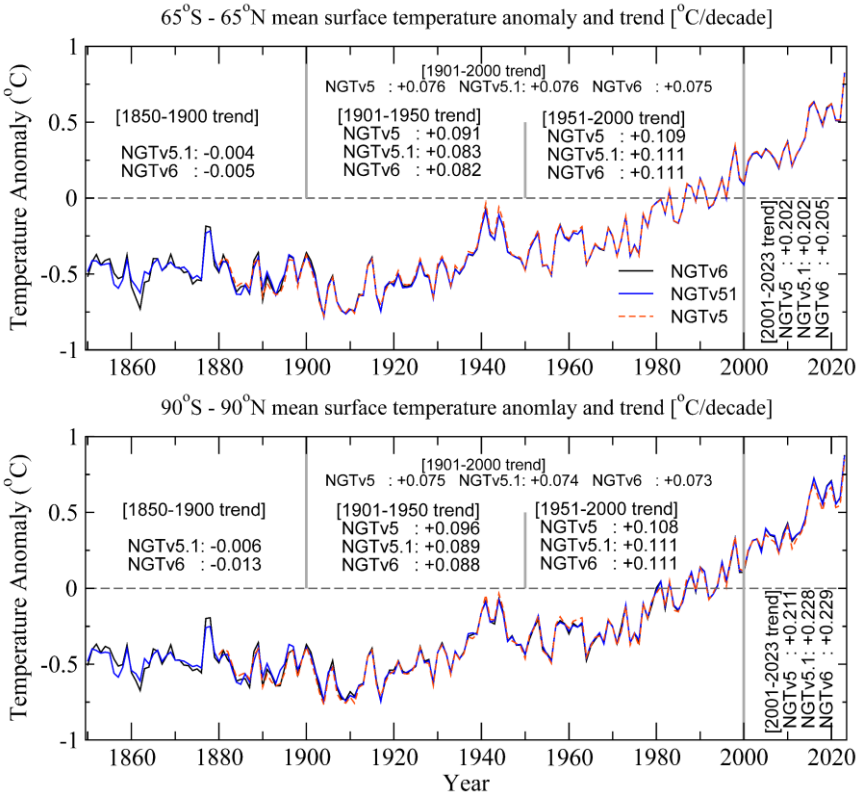

Fig. 3 Mean surface temperature anomalies for extrapolar (65°S–65°N; upper panel) and global (90°S–90°N; lower panel) regions derived from the three NOAAGlobalTemp versions—NGTv5, NGTv5.1, and NGTv6. Trends in units of °C/decade for selected periods are denoted in the figure.

Accepted for publication in *Bulletin of the American Meteorological Society*. DOI 10.1175/BAMS-D-24-0012.1.

Fig. 4 displays the NGTv6 trend at each grid for 1901−2000 and 2001−2023. In both periods, positive (warming) trends were predominant globally. Trends were mild during 1901−2000, mostly within ±0.1°C/decade. However, they intensified during 2001−2023, with trends ranging within ±0.5°C/decade in the Southern Hemisphere and frequently exceeding 0.5°C/decade in the Northern Hemisphere. In particular, trends in the two polar regions largely reversed between the two periods. In East Antarctica, trends were slightly positive during 1901−2000, but they turned negative during 2001−2023, reaching as low as -0.5°C/decade. In the Arctic Ocean, negative trends around -0.1°C/decade were observed during 1901−2000, but much higher positive trends (>1.5°C/decade) were seen during 2001−2023. Over the twenty-first century to date (2001−2023), the trend of the surface mean temperature for the Arctic region (poleward of 65°N) was 0.964°C/decade ($p \leq 0.01$), which is more than four times that of the entire global region (0.229°C/decade; $p \leq 0.01$). The trend patterns of NGTv5.1 (Fig. S2) and NGTv5.0 (Fig. S3; excluding the polar regions) are nearly identical to those of NGTv6.

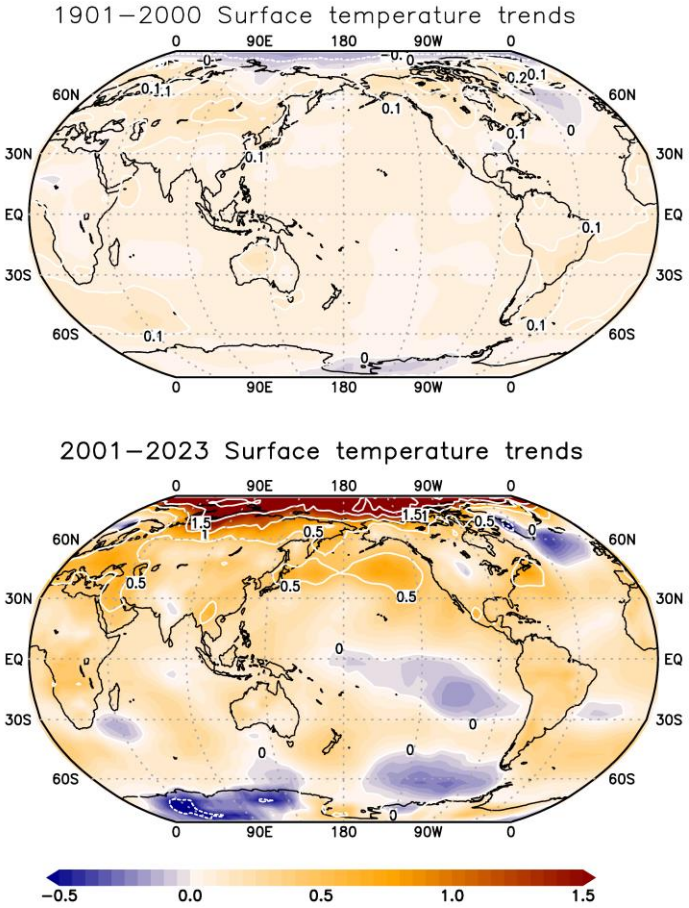

Fig. 4. NGTv6 surface temperature trends (units: °C/decade) during 1901−2000 and 2001−2023.

Accepted for publication in *Bulletin of the American Meteorological Society*. DOI 10.1175/BAMS-D-24-0012.1.

Overall, the large-scale spatial trend patterns shown here as well as the mean temperature variations shown in Fig. 3 are very similar among the three versions, despite improved data constructions in NGTv6. This is because, during the version updates, the underlying input data mostly remained the same and the low-frequency component of surface temperatures was reconstructed using the same method (Smith and Reynolds, 2005; Vose et al., 2021; Huang et al., 2022).

Summary

NOAAGlobalTemp has been updated to version 6, which involves enhancements in data and methodology over its previous major version. Full global coverage is achieved by using surface air temperature for the Arctic Ocean and removing the data reconstruction mask. An AI-based model is implemented for filling data gaps over the land and the Arctic Ocean. As of February 2024, the new version is available from the NOAA National Centers for Environmental Information.

ACKNOWLEDGMENTS

We thank the three anonymous referees for their insightful comments and suggestions. The graphics were generated using Grid Analysis and Display System (GrADS) and GRaphing, Advanced Computation and Exploration of data (GRACE).

DATA AVAILABILITY STATEMENT

The NOAAGlobalTemp data is openly available at: https://www.ncei.noaa.gov/products/land-based-station/noaa-global-temp.

References

Freeman, E., S.D. Woodruff, S.J. Worley, S.J. Lubker, E.C. Kent, W.E. Angel, D.I. Berry, P. Brohan, R. Eastman, L. Gates, W. Gloeden, Z. Ji, J. Lawrimore, N.A. Rayner, G. Rosenhagen, and S.R. Smith, 2017: ICOADS Release 3.0: A major update to the historical marine climate record. *Int. J. Climatol.* (CLIMAR-IV Special Issue), **37**, 2211-2237, https://doi.org/10.1002/joc.4775.

Hersbach, H., and Coauthors, 2020: The ERA5 global reanalysis. *Q. J. R. Meteorol. Soc.*, **146**, 1999− 2049, https://doi.org/10.1002/qj.3803

Accepted for publication in *Bulletin of the American Meteorological Society.* DOI 10.1175/BAMS-D-24-0012.1.

Huang, B., X. Yin, M. J. Menne, R. Vose, and H. Zhang, 2022: Improvements to the Land Surface Air Temperature Reconstruction in NOAAGlobalTemp: An Artificial Neural Network Approach. Artif. Intell. Earth Syst., **1**, e220032, https://doi.org/10.1175/AIES-D-22-0032.1.

Huang, B., P.W. Thorne, V. F. Banzon, T. Boyer, G. Chepurin, J.H. Lawrimore, M.J. Menne, T.M. Smith, R.S. Vose, and H.-M. Zhang, 2017: Extended Reconstructed Sea Surface Temperature version 5 (ERSSTv5), Upgrades, validations, and intercomparisons. *J. Climate*, **30**, 8179–8205, https://doi.org/10.1175/JCLI-D-16-0836.1.

Liu, C, E. Freeman, E.C. Kent, D.I. Berry, S.J. Worley, S.R. Smith, B. Huang, H.-M. Zhang, T. Cram, Z. Ji, M. Ouellet, I. Gaboury, F. Oliva, A. Andersson, W.E. Angel, A.R. Sallis, and A. Adeyeye, 2022: Blending TAC and BUFR Marine in Situ Data for ICOADS Near-Real-Time Release 3.0.2. *J. Atmos. Oceanic Technol.,* **39**, 1943–1959, https://doi.org/10.1175/JTECH-D-21-0182.1.

Menne, M.J., C.N. Williams, B.E. Gleason, J.J Rennie, and J.H. Lawrimore, 2018: The Global Historical Climatology Network Monthly Temperature Dataset, Version 4. *J. Climate*, **31**, 9835–9854, https://doi.org/10.1175/JCLI-D-18-0094.1.

Rigor, I.G., and M. Ortmeyer, 2003: The International Arctic Buoy Programme (IABP), *Proc. Eos Trans.* AGU, **84**(46), Fall Meet. Suppl., Abstract C41C-0987.

Serreze, M.C., and R.G. Barry, 2011: Processes and impacts of Arctic amplification: A research synthesis. *Glob. Planet. Change*, **77**, 85−96, https://doi.org/10.1016/j.gloplacha.2011.03.004.

Smith, T.M., and R.W. Reynolds, 2005: A Global Merged Land–Air–Sea Surface Temperature Reconstruction Based on Historical Observations (1880–1997). *J. Climate*, **18**, 2021–2036, https://doi.org/10.1175/JCLI3362.1.

Smith, T.M., R.W. Reynolds, T.C. Peterson, and J. Lawrimore, 2008: Improvements to NOAA's historical merged land–ocean surface temperatures analysis (1880–2006). *J. Climate*, **21**, 2283–2296, https://doi.org/10.1175/2007JCLI2100.1.

van den Dool, H. M., S. Saha, and Å. Johansson, 2000: Empirical Orthogonal Teleconnections. *J. Climate,* **13**, 1421–1435, https://doi.org/10.1175/1520-0442(2000)013<1421:EOT>2.0.CO;2.

Accepted for publication in *Bulletin of the American Meteorological Society.* DOI 10.1175/BAMS-D-24-0012.1.

Vose, R.S., B. Huang, X. Yin, D. Arndt, D.R. Easterling, J.H. Lawrimore, M.J. Menne, A. Sanchez-Lugo, and H.M. Zhang, 2021: Implementing Full Spatial Coverage in NOAA's Global Temperature Analysis. *GRL*, **48**, e2020GL090873, https://doi.org/10.1029/2020GL090873.

Vose, R.S., D. Arndt, V.F. Banzon, D.R. Easterling, B. Gleason, B. Huang, E. Kearns, J.H. Lawrimore, M.J. Menne, T.C. Peterson, R.W. Reynolds, T.M. Smith, C.N. Williams, Jr., and D.L. Wuertz, 2012: NOAA's merged land-ocean surface temperature analysis. *BAMS*, **93**, 1677–1685, https://doi.org/10.1175/BAMS-D-11-00241.1.

Zhang, H.-M., J. H. Lawrimore, B. Huang, M. J. Menne, X. Yin, A. Sanchez-Lugo, B. E. Gleason, R. Vose, D. Arndt, J. J. Rennie, and C. N. Williams, 2019: Updated temperature data give a sharper view of climate trends. *EOS*, **100**, https://doi.org/10.1029/2019EO128229.

Accepted for publication in *Bulletin of the American Meteorological Society*. DOI 10.1175/BAMS-D-24-0012.1.